ADVANCES IN ATMOSPHERIC SCIENCES, VOL. 24, NO. 5, 2007, 875–880

Measurements of Nighttime Nitrate Radical Concentrations in the Atmosphere by Long-Path Differential Optical Absorption Spectroscopy

LI Suwen*(李素文), LIU Wenqing (刘文清), XIE Pinhua (谢品华),
LI Ang (李 昂), QIN Min (秦 敏), and DOU Ke (窦 科)

Key Laboratory of Environmental Optical & Technology, Anhui Institute of Optics & Fine Mechanics, Chinese Academy of Sciences, Hefei 230031

(Received 25 July 2006; revised 31 October 2006)

ABSTRACT

The long-path differential optical absorption spectroscopy (LP-DOAS) technique was developed to measure nighttime atmospheric nitrate radical (NO_3) concentrations. An optimized retrieval method, resulting in a small residual structure and low detection limits, was developed to retrieve NO_3. The time series of the NO_3 concentration were collected from 17 to 24 March, 2006, where a nighttime average value of 15.8 ppt was observed. The interfering factors and errors are also discussed. These results indicate that the DOAS technique provides an essential tool for the quantification of NO_3 concentration and in the study of its effects upon nighttime chemistry.

Key words: nitrate radical, long-path differential optical absorption spectroscopy, detection limits, errors

DOI: 10.1007/s00376-007-0875-2

1. Introduction

The nitrate radical (NO_3) plays an important role as a catalyst within the complex nighttime atmospheric chemical system (Platt et al., 1990, 2002; Geyer et al., 1999, 2001, 2003; Allan et al., 1999). Due to its high reactivity and low atmospheric concentrations, the measurement of the concentration of NO_3 in the atmosphere is a challenge for any analytical technique (John and Chia, 1992; Carslaw et al., 1997; Geyer et al., 1999; Geyer et al., 2001; Mclaren et al., 2004).

Long-path differential optical absorption spectroscopy (LP-DOAS) (Platt et al., 1979) technique is based on the integrated absorption of ultraviolet (UV) and visible light along specific light path in the atmosphere over several kilometers by the nitrate radical as well as a number of other trace gases. DOAS uses the narrow molecular absorption bands to identify trace gases and their absorption strength to retrieve trace gases concentrations (Platt et al., 1979, 1990; Stutz and Platt, 1996; Xie et al., 2004; Si et al., 2006). The advantage of DOAS is its remote sensing capability, time resolution of typically a few minutes and the fact that it is a contact-free method, thereby preventing reactions on the surface of a sampler. Therefore, LP-DOAS is presented as a method for measuring the nighttime NO_3 concentration in the atmosphere and an optimized retrieval method was developed that provided good quantitative results.

2. Principle of the DOAS method

The process can be described as follows: light, with an intensity I_0, is emitted by a suitable source and passes through the open atmosphere. During its procession along its designed path, the light undergoes extinction due to absorption processes involving its interactions with various trace gases as well as due to scattering of air molecules and aerosol particles. The intensity I at the end of the optical path is given by Eq. (1) via Lambert-Beer's law (Stutz and Platt, 1996):

$$I(\lambda) = I_0(\lambda) \exp\left\{\sum_{i=1}^{n}[-\sigma_i(\lambda) - \sigma_i'(\lambda) -\right.$$

*Corresponding author: LI Suwen, swli@aiofm.ac.cn

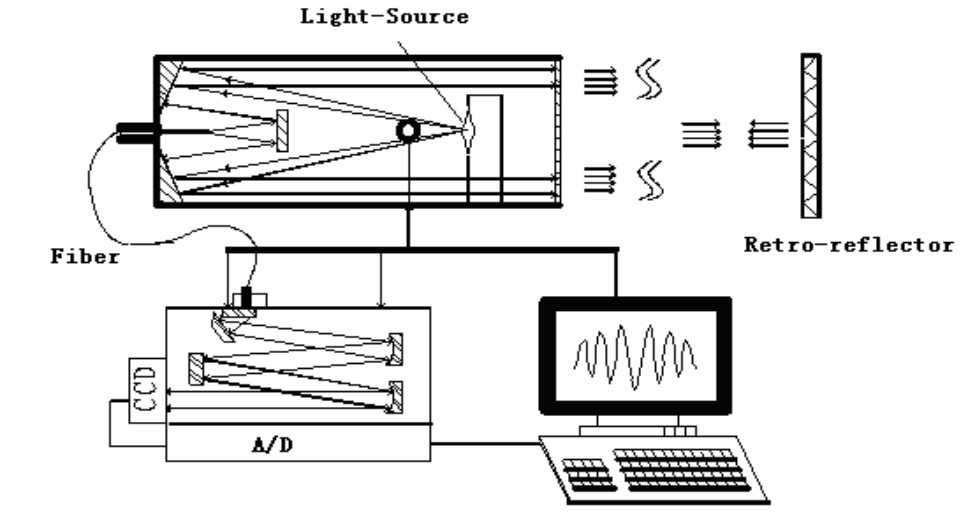

Fig. 1. Schematic view of the DOAS system.

$$\varepsilon_{\mathrm{R}}(\lambda) - \varepsilon_{\mathrm{M}}(\lambda)]N_i L \Big\} + B(\lambda) \,. \qquad (1)$$

Here, λ denotes the wavelength, L is optical path, n is the number of trace species. The differential cross section $\sigma_i(\lambda)$ represents the narrow spectral structures. $\sigma_i'(\lambda)$ denotes the broad spectral features, while N_i refers to the concentration. The Rayleigh and Mie extinctions due to aerosols are described by $\varepsilon_{\mathrm{R}}(\lambda)$ and $\varepsilon_{\mathrm{M}}(\lambda)$. $B(\lambda)$ is the noise that is dependant upon I. The logarithm of the ratio of the measured I_0 and I is given by Eq. (2):

$$\ln[I_0(\lambda)/I(\lambda)] = \sum_{i=1}^{n} [\sigma_i(\lambda) + \sigma_i'(\lambda) + \varepsilon_{\mathrm{R}}(\lambda) + \varepsilon_{\mathrm{E}}(\lambda)]N_i L + B'(\lambda) \,, \qquad (2)$$

where $\sigma_i'(\lambda), \varepsilon_{\mathrm{R}}(\lambda)$, and $\varepsilon_{\mathrm{M}}(\lambda)$ are the "slow" variations in the absorption spectra. A polynomial of a specified degree is then used to filter these "slow" variations out, leaving us with the optical density as defined below,

$$\ln(I_0/I) = \sum_{i=1}^{n} \sigma_i N_i L + B'(\lambda) \,. \qquad (3)$$

The concentration of various trace gases may be retrieved through the use of least-squares fitting of the reference spectra to the optical density.

3. Measurement algorithms for determining the NO_3 concentration

3.1 *Location*

The NO_3 radical was continuously observed by using a long-path DOAS instrument located at the western outskirts of Hefei (31°86′N, 117°23′E) from 17 to 24 March 2006. The monitoring site, located at the Anhui Institute of Optics & Fine Mechanics, was surrounded by trees and water, and in addition, the measuring station was situated approximately 15 m above the field. At a distance of 1.4 km, an array of 13 retro-reflectors was placed on another building.

3.2 *Measurement system*

The NO_3 radical concentration was measured along a 2.8 km optical path by using modified LP-DOAS. Figure 1 shows a schematic diagram highlighting the integral portions of the DOAS system. The measurement system included a 150 W high-pressure Xenon lamp. A Cassegrain telescope, with a focal distance of 645 mm and an aperture of 4, was used to transmit and receive the light. The reflecting system consisted

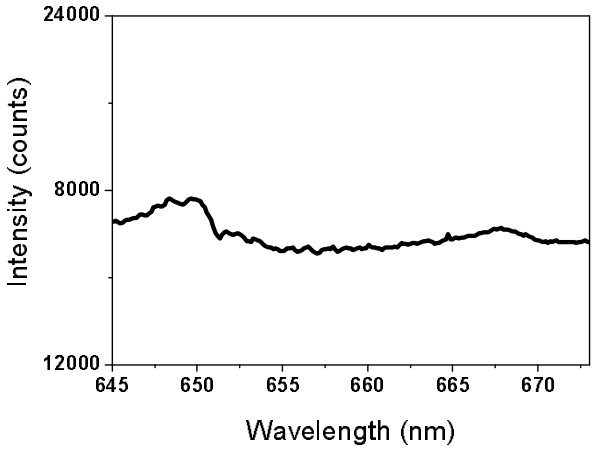

Fig. 2. A night time atmosphere spectrum in the region (645–670 nm).

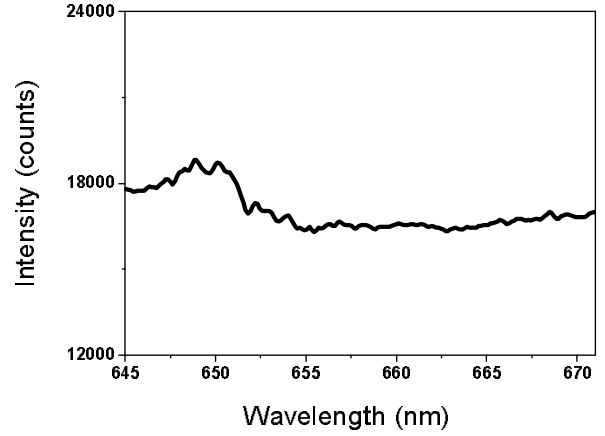

Fig. 3. A daytime reference spectrum in the region (645–670 nm).

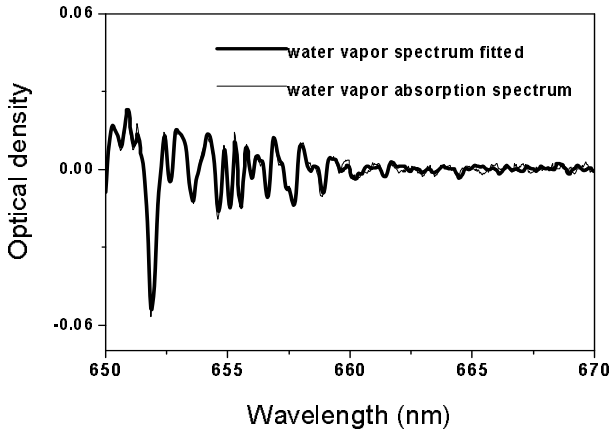

Fig. 4. A water vapor absorption fitted spectrum.

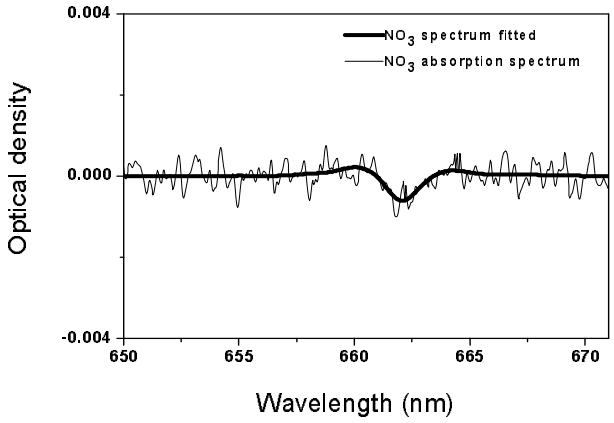

Fig. 5. An NO_3 absorption fitted spectrum with a concentration of 17.8 ppt.

of an array of thirteen retro-reflectors. A 610 nm long-pass filter was used to reduce the effects of stray light at shorter wavelengths, which was placed within the fiber coupler. A 7×0.2 mm diameter fiber bundle, which was regulated by a mode mixer to reduce unwanted structures, carried the incident light into the spectrometer (blaze wavelength: 500 nm, entrance slit: 100 m, dispersion: 6.2 nm mm^{-1}, spectral resolution: 0.42 nm, aperture: 4, stabilized at $30 \pm 0.2°C$). The Charge Coupled Device(CCD) detector, cooled to $-45°C$, was mounted in the focal plane of the spectrograph and the digital signal, which was transformed by a 16 bit A/D converter, was stored and analyzed using the computer.

4. Evaluation of NO_3

4.1 *Reference spectra*

The nitrate radical is detected in the red spectral range (Amekudzi et al., 2005; Geyer et al., 1999, 2003; Steven et al., 2005), with two absorption peaks being observed at 662 and 623 nm, which, in this study, were used to qualitatively identify the presence of NO_3 within each spectrum. The absorption feature centered at 662 nm, expanding over the 645–670 nm range, was used to quantify the NO_3 concentration. The cross-section, $\sigma(662\text{ nm})=2.25\times10^{-17}$ cm^2, was used for the NO_3 evaluation.

Apart from the NO_3 radical, the main absorbing medium in that region (645–670 nm) was water vapor (Noxon et al., 1980; Platt et al., 1980). The influence of water is critical in the evaluation of the NO_3 concentration, because overtone bands due to the presence of water vapor peak at 651.5 nm, which is very close to the main line for NO_3, and furthermore, the optical density of water vapor is not linearly dependent on the optical path. However, the concentration of NO_3 during the daytime is negligible due to its rapid photolysis (lifetime is only 5 s) (Geyer et al., 1999; Vrekoussis et al., 2004; Mihelcic et al., 1993). Therefore, daytime atmospheric absorption spectra (at solar zenith angles$<80°$) can serve as reference spectra for determining the background water absorption.

The best results were achieved using two daytime spectra (sunrise and sunset at solar zenith angles$<80°$) that were recorded close to the studied night. In addition, the offset, dark-current spectra and stray light were also recorded to allow corrections to the measured spectra used in this work.

4.2 NO_3 *spectral fitting process*

In the first step, the measured atmospheric spectra were corrected to compensate for the effects due to

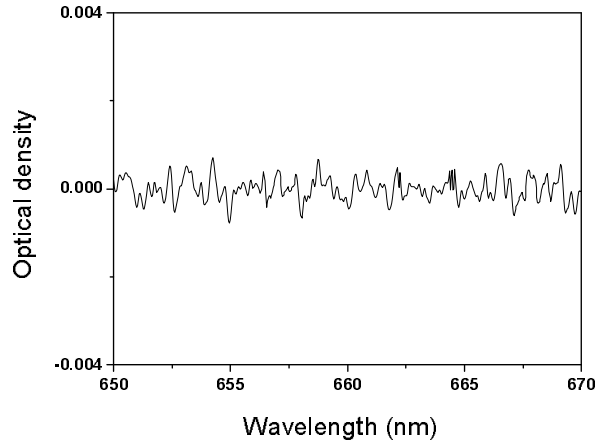

Fig. 6. A residual spectrum.

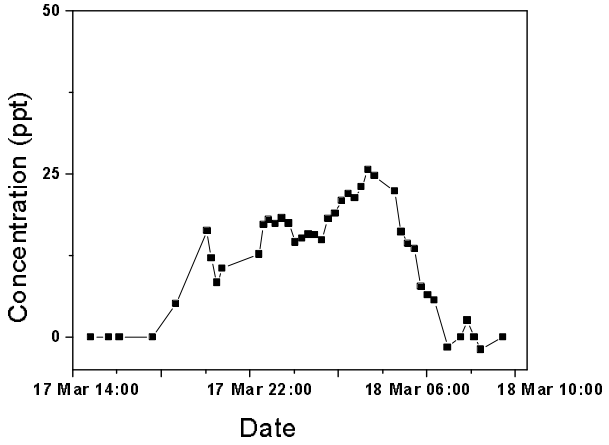

Fig. 7. The diurnal profile of the NO_3 concentration from 1400 LST 17 March to 1000 LST 18 March.

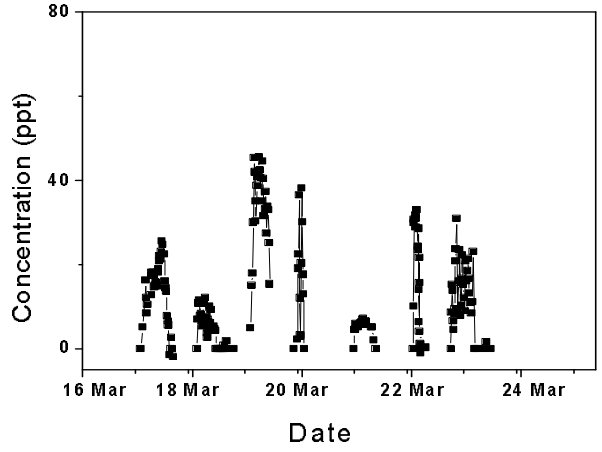

Fig. 8. Time series of the NO_3 concentration at Hefei from 17 to 24 March 2006.

stray light, the electronic offset and the dark current. The logarithm of the resulting spectrum was then numerically high-pass filtered, with a subsequent low-pass filtering of the result. Therefore, high-frequency noises, as well as the broadband extinction structure, were greatly reduced. The water vapor reference spectra were obtained by interpolating two daytime atmospheric references. Then the reference spectra for NO_3 and water vapor were fitted to the measured spectrum simultaneously based on a least squares fitting routine after they were subjected to the aforementioned filtering technique.

Figures 2–6 illustrate examples of the NO_3 concentration evaluation. A night time atmosphere spectrum and a daytime water vapor reference spectrum are presented in Figs. 2 and 3, respectively. The water vapor absorption band (see Fig. 4) was then subtracted from the night time atmosphere spectrum, thereby allowing the NO_3 absorption band at 662 nm to appear more clearly (Fig. 5), in this case corresponding to a concentration of 17.8 ppt. Finally, the residual spectrum was illustrated in Fig. 6. The RMS residual was found to be less than 1×10^{-4}.

NO_3 concentration profiles that were collected on the night of 17–18 March 2006 are shown in Fig. 7. These profiles indicate that the effects of the daytime photolysis of NO_3 are clearly apparent at both sunset and sunrise. The maximum value of 26.8 ppt was observed at 0404 LST on the morning of 18 March. Figure 8 presents a time series of the NO_3 concentration at the western outskirts of Hefei from 17 to 24 March 2006. The daily maximum value for the NO_3 concentration varied from 9.7 ppt to 47.6 ppt, with the average level falling at 15.8 ppt.

5. Detection limits and errors

5.1 *Detection limits*

The detection limits of a DOAS system are directly proportional to the differential optical density, τ_{res}, of the residual structure, while inversely proportional to the optical path length, L, and the differential cross-section, $\delta_{(\sigma)}$, therefore, it can be calculated via Eq. (4) (Qin et al., 2005),

$$C_{\min} = \frac{\tau_{\mathrm{res}}}{\delta_{(\sigma)} \cdot L} \tag{4}$$

where, $\delta_{(\sigma)}$ is the differential cross-section of NO_3. Therefore, the detection limits of the system used in this work for NO_3 detection was 3.8 ppt.

5.2 *Errors*

The errors associated with the DOAS system included experimental system error, the reference cross-

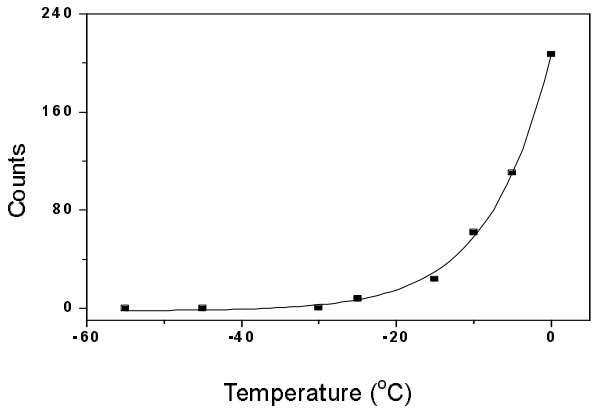

Fig. 9. Relationship between temperature and the dark current.

section error of NO_3 and the error due to the least squares fitting procedure. Experimental error consisted of the influence of the dark current and the offset of the CCD, ambient stray light, and the small shift in the spectral dispersion across the pixels. Figure 9 shows the relationship between the dark current and the temperature. It was found that lower temperatures resulted in smaller dark currents, as might be expected. Therefore, the CCD was cooled to $-45°C$ in an effort to reduce the dark current as much as possible. As for offset and stray light, these were experimentally measured and were then used to correct the raw spectra. In order to minimize thermal misadjustments, the whole spectrograph unit was thermally isolated and thermo-stated to $(30 \pm 0.2)°C$ by a PID controller. Thus the experimental error was estimated to fall below 2%.

The standard cross-section of the NO_3 radical was difficult to determine precisely. Various studies of the wavelength and temperature dependences of NO_3 concentrations have been performed over the past few years. While most of the studies reported have achieved similar relative spectral shapes, there were discrepancies concerning the absolute value of the absorption cross-section. A recent publication (Amekudzi et al., 2005) that was focused on measuring the NO_3 cross-section yielded a value of $(2.23\pm0.22) \times 10^{-17}$ cm^2, which can be found at http:// www. atmosphere.mpg.de. The value for the cross-section of $\sigma(662 \text{ nm})=2.25 \times 10^{-17}$ cm^2 was used for the NO_3 concentration evaluations here in this work. The cross-section error was estimated to be below 8%.

The error of the least squares fitting procedure, which underestimates the "true" statistical error (1σ), must be corrected by a factor of 3. So the fitting error in the determination of the NO_3 concentration was found to be approximately 8%.

The whole error, which was calculated by Gaussian error transfer expressions, was found to be about 11.5%, while the given error of Geyer was 14%.

6. Conclusions

Using the LP-DOAS method, we have taken the lead in measuring nighttime atmospheric NO_3 concentrations at Hefei, with the concentrations that were measured over an entire week being provided. By optimized the retrieval method, the detection limits were able to reach 3.8 ppt with an optical path of 2.8 km, and furthermore, the total systematic error was reduced to 11.5%. This indicates that the DOAS method is an essential tool for the quantification of the NO_3 concentration and for studying nighttime atmospheric chemistry.

Acknowledgements. The authors would like to thank the DOAS group for their help. This project was financially supported by the National High Technology Development Program of China (Grant No. 2005AA641010)

REFERENCES

Allan, B. J., N. Carslaw, H. Coe, R. A. Burgess, and J. M. C. Plane, 1999: Observation of nitrate radical in the marine boundary layer. *Journal of Atmospheric Chemistry*, **33**, 129–154.

Amekudzi, L. K., B. M. Sinnhuber, and N. V. Sheode, 2005: Retrieval of stratospheric NO_3 vertical profiles from SCIMACHY lunar occultation measurement over the Antarctic. *J. Geophys. Res.*, **110**(D20304), doi: 10.1029/2004JD005748.

Carslaw, N., L. J. Carpenter, J. M. C. Plane, B. J. Allan, R. A. Burgess, K. C. Clemitshaw, H. Coe, and S. A. Penkett, 1997: Simultaneous observations of nitrate and peroxy radicals in the marine boundary layer. *J. Geophys. Res.*, **102**, 18917–18933.

Geyer, A., B. Alicke, D. Mihelcic, J. Stutz, and U. Platt, 1999: Comparison of tropospheric NO_3 radical measurements by differential optical absorption spectroscopy and matrix isolation electron spin resonance. *J. Geophys. Res.*, **104**(D21), 26097–26105.

Geyer, A., B. Alicke, S. Konrad, T. Schmitz, J. Stutz, and U. Platt, 2001: Chemistry and oxidation capacity of the nitrate radical in the continental boundary layer near Berlin. *J. Geophys. Res.*, **106**(D8), 8013–8025.

Geyer, A., and Coauthor, 2003: Direct observation of daytime NO_3: Implications for urban boundary layer chemistry. *Geophys. Res. Lett.*, **108**(D12), 4368, doi: 10.1029/2002JD002967.

John, M. C. P., and F. N. Chia, 1992: Differential optical absorption spectrometer for measuring atmospheric trace gases. *Review of Scientific Instrument*, **63**(3), 1867–1875.

Mclaren, R., A. S. Rhian, L. John, L. H. Katherine, G.

A. Kurt, and L. Richard, 2004: Nighttime chemistry at a rural site in the Lower Fraser valley. *Atmos. Environ.*, **38**, 5837–5848.

Mihelcic, D., D. Klemp, P. Müsgen, H. W. Päsgen, and A. V. Thomas, 1993: Simultaneous measurements of peroxy and nitrate radical at Schauinsland. *Journal of Atmospheric Chemistry*, **16**, 313–335.

Noxon, J. F., R. B. Norton, and E. Marovich, 1980: NO_3 in the troposphere. *Geophys. Res. Lett.*, **7**, 125–128.

Platt, U., D. Perner, and H. Patz, 1979: Simultaneous measurements of atmospheric CH_2O, O_3, NO_2 in the polluted troposphere by differential optical absorption. *J. Geophys. Res.*, **84D**, 6329–6335.

Platt, U., D. Perner, G. W. Harris, A. M. Winer, and J. M. Pitts, 1980: Detection of NO_3 in the polluted troposphere by differential optical absorption. *J. Geophys. Res.*, **7**, 89–92.

Platt, U., G. Lebras, G. Poulet, J. P. Burrows, and G. K. Moortgat, 1990: Peroxy radicals from night-time reaction of NO_3 with organic compounds. *Nature*, **348**, 147–149.

Platt, U., and Coauthors, 2002: Free radicals and fast photochemistry during BERLIOZ. *Journal of Atmospheric Chemistry*, **42**, 359–394.

Qin, M., and Coauthors, 2005: Study on UV-visible DOAS System Based on Photodiode Array (PDA). *Spectroscopy and Spectral Analysis*, **25**(9), 1463–1467.

Si, F. Q., J. G. Liu, P. H. Xie, Y. J. Zhang, W. Q. Liu, H. Kuza, N. Lagrosas, and N. Takeuchi, 2006: Correlation study between suspended particulate matter and DOAS data. *Adv. Atmos. Sci.*, **23**(3), 461–467.

Stutz, J., and U. Platt, 1996: Numerical analysis and estimation of the statistical error of differential optical absorption spectroscopy measurements with least-squares methods. *Appl. Opt.*, **35**(30), 6041–6053.

Steven, S. B., and Coauthors, 2005: Aircraft observations of daytime NO_3 and N_2O_5 and their implications for tropospheric chemistry. *Journal of Photochemistry and Photobiology A: Chemistry*, **176**, 270–278.

Vrekoussis, M., and Coauthors, 2004: Role of the NO_3 radicals in oxidation processes in the eastern Mediterranean troposphere during the MINOS campaign. *Atmospheric Chemistry and Physics*, **4**, 169–182.

Xie, P. H., W. Q. Liu, Q. Fu, J. G. Liu, and Q. N. Wei, 2004: Intercomparison of NO_x, SO_2, O_3 and aromatic hydrocarbons measured by a commercial DOAS system and traditional point monitoring techniques. *Adv. Atmos. Sci.*, **21**(2), 211–219.